Available online at www.sciencedirect.com
ScienceDirect
New Astronomy Reviews 50 (2006) 984–992
New Astronomy Reviews
www.elsevier.com/locate/newastrev

The QUaD experiment

C. Pryke

Kavli Institute for Cosmological Physics, Department of Astronomy and Astrophysics, The Enrico Fermi Institute, University of Chicago, 5640 S. Ellis Avenue, Chicago, IL 60637-1433, USA

Available online 7 November 2006

For the QUaD Collaboration.

Abstract

QUaD is a 31 pixel array of polarization sensitive bolometer pairs coupled to a 2.6 m Cassegrain radio telescope. The telescope is attached to the mount originally built for the DASI experiment and located at the South Pole. The telescope system is described along with details of instrumental characterization studies which we have performed. A first season of CMB observations is complete and the second season underway. Details of the current status of these observations and their analysis are presented.

Keywords: Cosmic microwave background; Polarization

Contents

E-mail address: pryke@oddjob.uchicago.edu.

1387-6473/$ - see front matter © 2006 Published by Elsevier B.V.
doi:10.1016/j.newar.2006.09.030

1. Introduction

The past decade has seen an explosion in our understanding of the birth and evolution of the Universe in which we find ourselves, and we now have a detailed "standard cosmological model" known as LCDM. A central piece of the evidence for this model is the existence and detailed properties of the Cosmic Microwave Background (CMB)—a relic radiation field which comes to us from a time approximately 400,000 years after the beginning, when our expanding, cooling Universe made the transition from an opaque plasma to transparent gas—an event called "recombination". The anisotropy of the CMB traces the density structure at the time of recombination and the spatial characteristics of the pattern have been shown to be in excellent agreement with the predictions of the LCDM model. This model also predicts that the CMB should be polarized at a level ~10%, and further that there should be a nearly deterministic relationship between the unpolarized and polarized angular power spectra (Hu and White, 1997).

Although wildly successful in terms of agreement with detailed experimental results the LCDM model is deeply uncomfortable. In addition to including a ~30% contribution to the current energy density of the Universe in the form of mysterious collision-less dark matter, it also requires that empty space itself have an energy density—the so called dark energy. Given this seeming paradox of a well developed model which seems able to pass all the available tests, and the gaping hole in our understanding which this model represents we are compelled to test the model in all available ways—the quest to measure CMB polarization is central amongst these efforts.

One can decompose a polarization pattern into two scalar fields dubbed the *E*-mode (curl free) and *B*-mode (all curl) components. Fig. 1 shows the relationship between the various CMB power spectra. The same density fluctuations which give rise to the total intensity (T) anisotropy also produce *E*-mode polarization anisotropy. The intensity anisotropy is caused directly by the density fluctuations while the polarization anisotropy is caused primarily by the motions of material induced by these variations in density. This distinction is what causes the peaks of the E spectrum to be anti-phase with respect to the T spectrum. Because the motions occur along the density gradients the intrinsic polarization pattern is curl free—pure *E*-mode. The CMB travels to us through evolving large scale structure which gravitationally lenses the radiation distorting the pattern and producing a small "lensing-B" component. Re-scattering of the CMB after the Universe re-ionizes causes modification of these spectra at large angular scales (smaller ℓ number) as shown by the dotted lines in the figure.

LCDM does not depend explicitly on how the Universe came to be, assuming only the simplest possible initial conditions at some very early time (scale free adiabatic perturbations). Inflation is a very popular class of theories which naturally produce such conditions. A generic prediction of

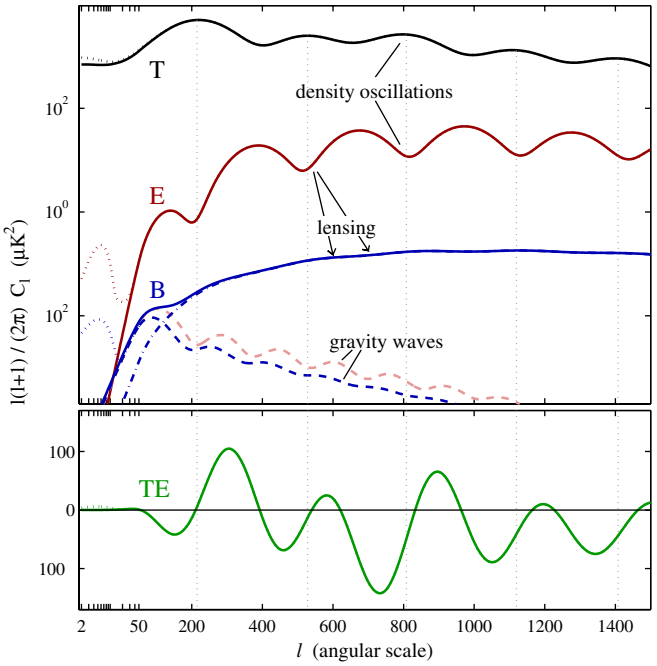

Fig. 1. The angular power spectra of the CMB—see text for details (figure courtesy of J. Kovac).

inflationary models is the existence of tensor perturbations propagating through the Universe. Such perturbations would produce both *E* and *B*-mode polarization anisotropy. While the *E*-mode contribution would be swamped below the density induced *E*, the inflationary *B*-modes *might* be detectable above the lensing-B at ℓ numbers around 100.

We have then the motivation for measuring the polarization anisotropy of the CMB: at $\ell < 30$ to constrain reionization, at $30 < \ell < 100$ to look for inflation, and at $\ell > 100$ to aggressively test the LCDM paradigm and gain information about large scale structure through lensing (see below).

It is often stated that measuring polarization is worthwhile not just to test LCDM, but also to increase the accuracy with which its parameters can be constrained. However as has been demonstrated by the Boomerang group (MacTavish et al., 2006) polarization data of modest quality at $\ell > 100$ adds little when considering the vanilla LCDM model. If one believes in LCDM it probably makes more sense to push measurements of T at high ℓ rather than to measure *E*-mode polarization. If lensing-B can be detected the situation changes since our lack of knowledge of the neutrino mass translates into a factor ~2 uncertainty in the expected level of lensing-B.

The Polarization of the CMB was first detected by the 30 GHz radio interferometer DASI operating at South Pole (Kovac et al., 2002). DASI made a convincing detection of *E*-mode polarization in the ℓ range of a few hundreds, and also TE cross correlation in the same range. Shortly thereafter the WMAP experiment announced results on TE at low ℓ. We now have measurements of

the *E* and *TE* spectra from CBI, Capmap, B2K and second releases from DASI and WMAP. As we see in Fig. 2 the current situation is that the first few peaks of the *E*-mode spectrum are starting to becomes clear and everything continues to look good for the standard LCDM expectation.

The QUaD experiment is optimized for polarization measurements at $\ell > 100$, and so as explained above is focused on testing the LCDM paradigm. With several years of data a low significance detection of lensing-B may become possible. In this paper we describe the QUaD telescope and the current status of the observations and data analysis. In Section 2 the telescope system and basic observing strategy is outlined. Section 3 gives details of some of the instrumental characterization studies we have done. Finally Section 4 describes the current status of the CMB observations and analysis.

2. The QUaD experiment

After four years of operation the DASI experiment was decommissioned. During the last year of its operation the DASI team was approached by a group already engaged in building a CMB polarization receiver and associated optics called QUEST with a view to putting these on the DASI mount at South Pole. A new collaboration called QUaD for "QUEST and DASI" was formed and work started on coupling the receiver and optics to the mount.

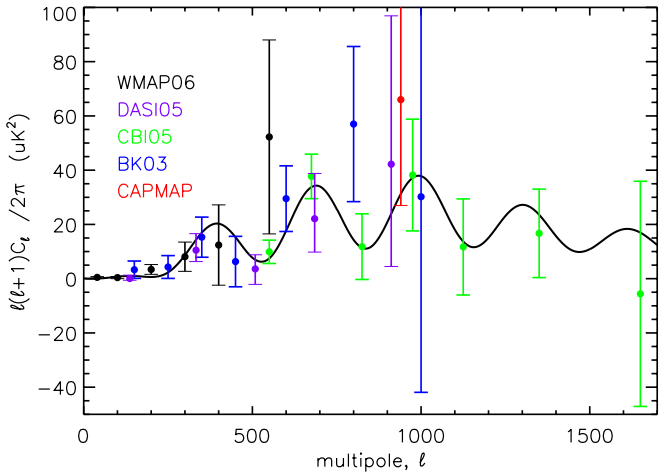

Fig. 2. Current results on the *E*-mode power spectrum of the CMB.

The QUaD experiment is a 31-pixel polarization-sensitive bolometric camera mounted on a 2.6 m Cassegrain radio telescope (Cahill et al., 2004). QUaD observes the CMB in two frequency bands nominally centered at 100 and 150 GHz. At these frequencies the South Pole site provides outstanding atmospheric conditions (Bussmann et al., 2005) and has provided ground-breaking CMB measurements through experiments such as DASI and ACBAR (Kuo et al., 2004).

2.1. Telescope

The telescope mount is altitude-azimuth with a third axis which allows the entire telescope to be rotated about the line-of-sight. Absolute pointing is under 1′ rms. The secondary mirror is supported by a one piece cone made from a foam which is almost perfectly RF transparent (Zotefoam) to minimize stray reflections that would otherwise arise from solid feed legs. The Cassegrain focus is coupled to the focal plane by two polyethylene lenses cooled to 4 K, and anti-reflection coated with Teflon. A picture of the QUaD telescope in its ground shield, and a schematic of the telescope, receiver and mount, are shown in Fig. 3.

2.2. Focal pane

The QUaD focal plane (Fig. 4) is equipped with 31 polarization-sensitive pixels, 19 at 150 GHz and 12 at 100 GHz. Each pixel comprises two polarization-sensitive bolometers (PSBs) mounted at the back of a corrugated feed-horn. Each bolometer, fabricated at the Jet Propulsion Laboratory (JPL), consists of a NTD Ge thermistor mounted on a silicon-nitride substrate that is etched and metalized to be sensitive to only one direction of linear polarization. These bolometers were developed for the Planck satellite and are also used in the Boomerang and BICEP experiments (Jones et al., 2003). Differencing the

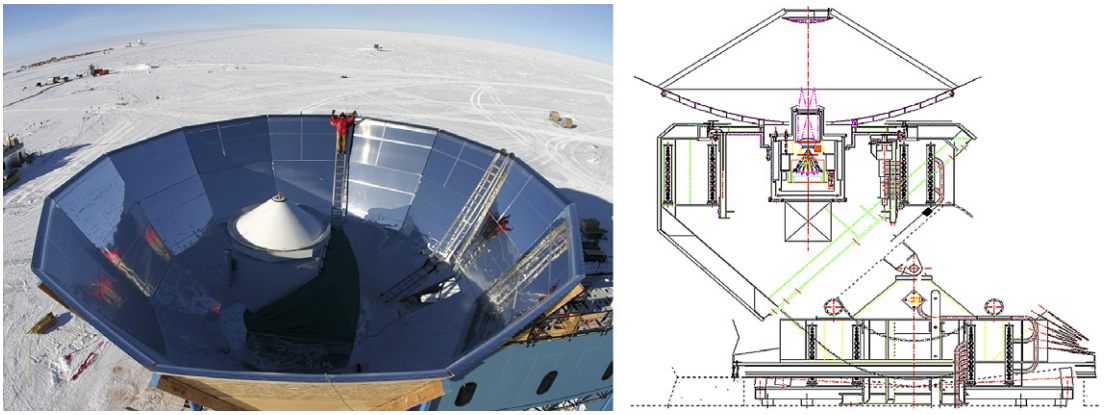

Fig. 3. Left: The QUaD telescope inside its ground shield at the South Pole Station. Right: Schematic of the telescope optics and receiver on the mount.

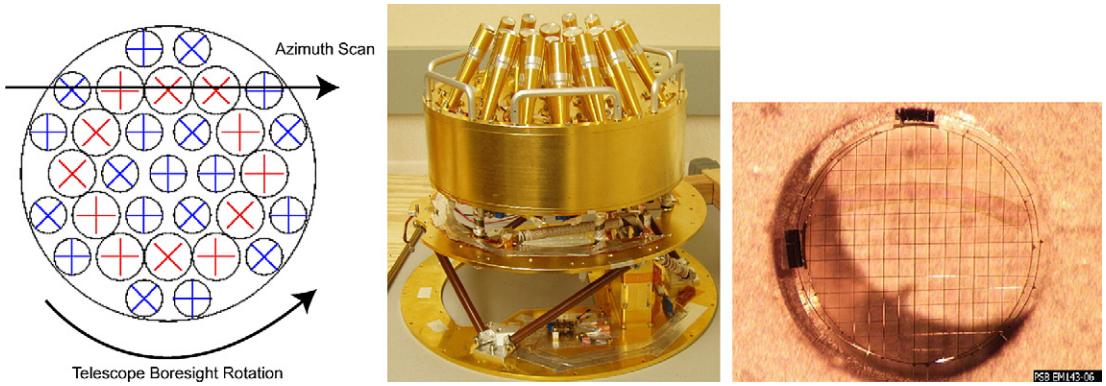

Fig. 4. The QUaD focal plane (center) contains 31 polarization-sensitive pixels, as shown in the schematic at left—the red (larger) pixels are 100 GHz, the blue (smaller) are 150 GHz and the crosses indicate the directions of polarization to which each PSB is sensitive. At right is a photograph of an individual PSB. (For interpretation of the references to color in this figure legend, the reader is referred to the web version of this article.)

Table 1
QUaD parameters as measured in the first season

	100 GHz	150 GHz
Bandwidths (%)	28	27
Beam sizes (arcmin)	5.6	4.5
Number of pixels[a]	12 (10)	19 (16)
Polarization sensitivity[b] (μK s$^{1/2}$)	380	350

[a] The number in brackets is the number of operational pixels in the 2005 (first) season.
[b] To Q or U, depending on the orientation of the pixel with respect to the chosen coordinate system.

signals from each of the bolometers in a single feed gives a measurement of Stokes parameter Q or U, depending on the orientation of the detector pair with respect to the chosen coordinate system. A waveguide throat inside the feeds defines the low-frequency band edge and resonant filters (Lee et al., 1996) at the feed aperture define the high-frequency edge. The measured performance parameters are summarized in Table 1.

2.3. Telescope scanning

QUaD observes by scanning the telescope in azimuth sweeping the focal plane across the sky as indicated in the left panel of Fig. 4. Azimuthal scanning minimizes changes in atmospheric emission that would otherwise cause a changing baseline during a scan (typical scan rates are of order 0.25° s^{-1}). The telescope is scanned several times at a given elevation (equivalent to declination at Pole), then stepped in elevation and the scans repeated to build up a "raster map" of the sky. As seen in Fig. 4 the pixels are of two orientation flavors—to increase the number of angles at which measurements are made the third axis of the mount is used to rotate the entire telescope assembly (primary, secondary and receiver) about the line of sight.

Because there is no sky rotation at the Pole, constant elevation scans provide no cross-linking of the map. Although this results in maps with anisotropic filtering our simulations demonstrate that this is *no impediment* to an un-biased reconstruction of the CMB power spectrum.

3. Instrument performance and characterization

In this section we demonstrate from first-season measurements that QUaD has the required stability and freedom from systematics to make accurate measurements of CMB polarization.

3.1. Gain calibration and stability

Sensitive measurements of CMB polarization using PSB pair differencing require that the relative gain of the two detectors in each pair be extremely stable. Our primary method of relative calibration is to nod the telescope every ten minutes by one degree in elevation, injecting an atmospheric ramp into the timestream (we call this an "elnod"). This provides a "beam filling" calibration source that varies in a known manner ($\sec\theta$) and is unpolarized to high precision. We find that the relative gains measured through this method are extremely stable and we use this method both for relative calibration within each pair, and also between pairs.

To further monitor gain stability we use a calibration source hidden behind the secondary mirror with a battery-operated flip mirror, controlled via an IR link. The source comprises an eccosorb black-body viewed though a rotating polarizing grid. The injected signal produces a sinusoidal modulation of the PSB output voltage. We find the fitted amplitudes of these sine waves to have excellent absolute stability over a period of months indicating that both the calibration source itself, and the receiver system are extremely stable. There is a small variation in absolute gain which correlates with atmospheric opacity and is easily understood as bolometer gain variation due to changes in optical loading. Hence, as expected, taking the modulation amplitude ratio within each PSB pair the stability is further increased. Fig. 5 shows that the relative gains of the detector pairs remain stable to better than 1% over the entire season.

Instrumental polarization (the conversion of an unpolarized input signal to a partially linearly polarized signal)

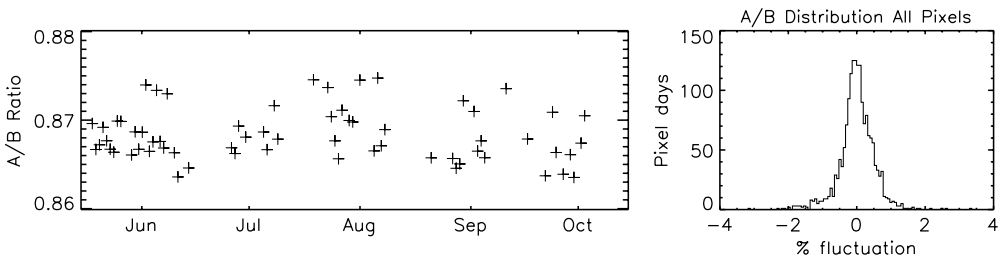

Fig. 5. The QUaD calibration source provides a frequent monitor of the gain stability for each detector. The ratio of the signals within a single PSB pair is shown at left (the A/B ratio). The RMS fluctuation of these A/B ratios for all detectors over all days in season 1 is 0.5% (right). This figure bins the histograms from all 31 pixels so the total number of histogram entries is the number of pixels times the number of days.

is indistinguishable in QUaD data from a relative gain difference between the two PSB halves. Thus Fig. 5 shows that both instrumental polarization and relative gain are extremely stable.

3.2. Atmospheric rejection

Ground-based measurements of CMB temperature anisotropies are subject to $1/f$ contamination from atmospheric emission fluctuations. Because these fluctuations are unpolarized, they are removed from our polarization measurements by differencing the two halves of the PSB. This is illustrated in Fig. 6 which shows five minutes of raw data from a QUaD detector pair.

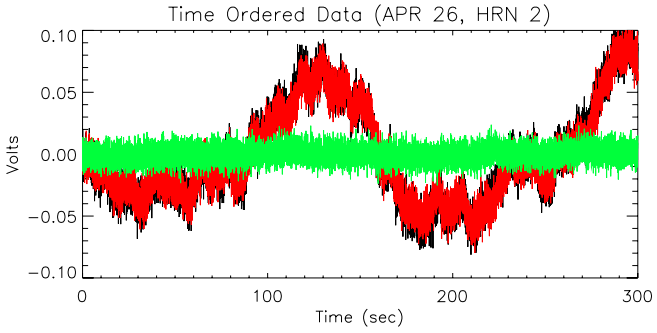

Fig. 6. Raw timestream from the two detectors in a single QUaD pixel (red and black traces) and the polarization measurement formed from the difference (green trace). Large excursions due to atmospheric noise are present but because they are almost completely common mode they cancel to high precision in the difference. (For interpretation of the references to color in this figure legend, the reader is referred to the web version of this article.)

3.3. Beam maps

The beam patterns and feed offset angles of QUaD are determined by mapping bright, un-polarized, galactic sources such as RCW38. Fig. 7 shows the result for a single detector from three such runs. QUaD was intended to have a fully steerable, computer-controlled hexapod mount for the secondary but, during commissioning, the mechanism was found to have unsatisfactory performance and was replaced before the start of first season observations with a fixed mount with manually adjustable set screws. The beams initially proved to have a large degree of ellipticity. This was due to a warp of about 100 μm across the primary mirror combined with being several mm from best focus. A manual re-focus was performed mid season leading to a considerable improvement, and for the second season a corrective secondary has been installed resulting in negligible residual ellipticity. For the second season we have also added a simple remote controlled focusing mechanism.

3.4. Characterization of polarization angles and efficiencies

Each QUaD feed contains two nominally orthogonal bolometers. To measure the polarization response of each

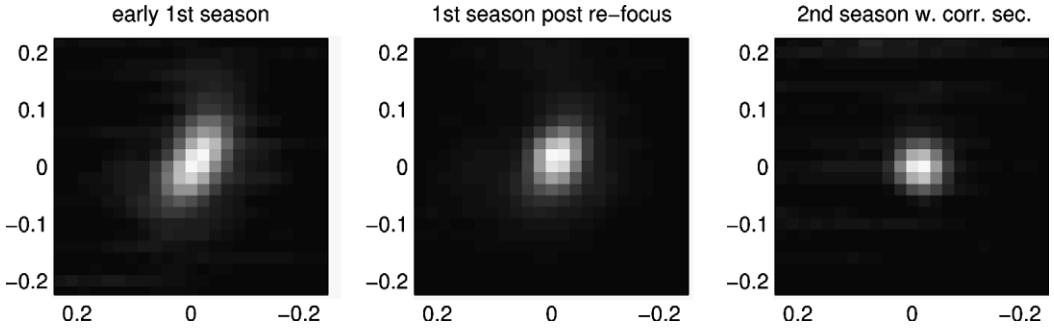

Fig. 7. Beam maps for a single QUaD detector made using the compact galactic source RCW38. At left we see the beam as it was early in the 1st season, showing strong ellipticity; the middle panel shows the result after the manual refocus described in the text. The right-hand panel shows that in the second season we have effectively eliminated ellipticity by installing a specially shaped secondary which corrects for the small warp of the primary.

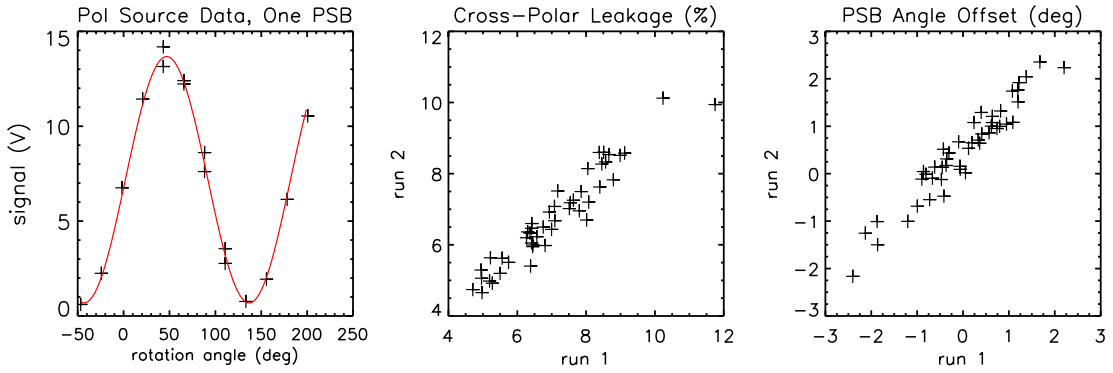

Fig. 8. (left) Data from the external polarized calibration source for a single PSB, from which cross-polar leakage and PSB orientation angle are derived (see text). (right) Comparison of this data for all detectors between two different calibration runs (one month apart) shows the stability of the polarization properties of the instrument.

detector a modulated source of linear polarization is used with two grids, one fixed and the other rotating, in front of an eccosorb black-body. By "locking-in" on the known angle of the rotating grid one can measure the response as a function of the angle of the fixed grid. The left panel of Fig. 8 shows the results of such a test. The phase of the sinusoid is determined by the absolute angle of the bolometer grid and the amount by which the troughs fail to reach zero is a measurement of the cross-polar leakage.

The polarization properties of the receiver alone were measured in the laboratory prior to deployment. The mean values of the cross-polar leakage were found to be about ~5% at 150 GHz and ~8% at 100 GHz, with a pixel–pixel scatter of about 3%, and the angles of the bolometers were found to be in good agreement with the design values.

Between seasons 1 and 2 we made in situ measurements of the complete telescope system using an external calibration source mounted on a tower outside the ground shield. Because this is a near-field measurements, collaborators at Maynooth College, Ireland modeled the propagation of the beam to show that the polarization efficiency and angle obtained by integrating over the near field pattern are identical to the far field values. The results of the near field measurements are in good agreement with the lab measurements indicating that the effects of the telescope are negligible. Fig. 8 compares two sets of polarization calibration observations made one month apart and shows excellent stability.

As a check on our ability to measure polarization, we have made maps of the moon. At these frequencies, scattering of thermal radiation as it leaves the lunar surface leads to a weak radial polarization pattern. Mapping the moon with QUaD is challenging because the moon does not rise sufficiently high above the horizon at South Pole to clear the ground shield, and also because the very strong emission causes significant detector saturation. Fig. 9 demonstrates that we can achieve precision measurements of polarization at the 1% level under very challenging conditions.

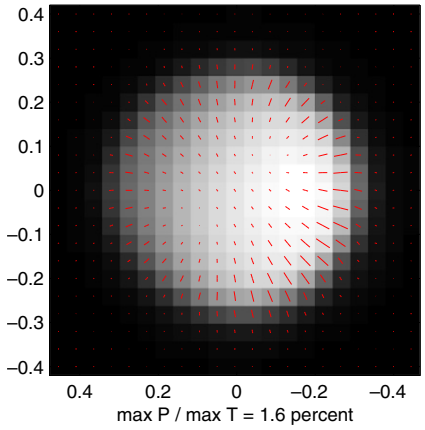

Fig. 9. QUaD polarization map of the moon at 150 GHz. The grayscale shows the lunar temperature, with polarization magnitude and direction indicated by the length and orientation of the overplotted lines. Note that the strongest polarization occurs around the limb and is of order 1%.

4. CMB observations

QUaD was commissioned at the South Pole from November 2004 to April 2005 and completed its first season of observation in October 2005.

4.1. Ground pickup

As discussed in Section 2, QUaD observes by scanning in azimuth. Each scan covers 7.5° which, because we observe a field centered at a declination of −47, corresponds to a scan length of 5° on the sky. We observe two fields separated by 0.5 h in RA to give ourselves the option of using the standard technique of lead-trail differencing to remove any ground pickup signal. Ground pickup is observed, and is correlated with the amount of snow accumulated on the ground-shield. The pickup is largely unpolarized but there is a small polarized component whose amplitude is not clearly correlated with the amount of snow. Although the pickup varies from day to day it appears to be highly stable over the half hour repeat timescale as lead-trail differencing

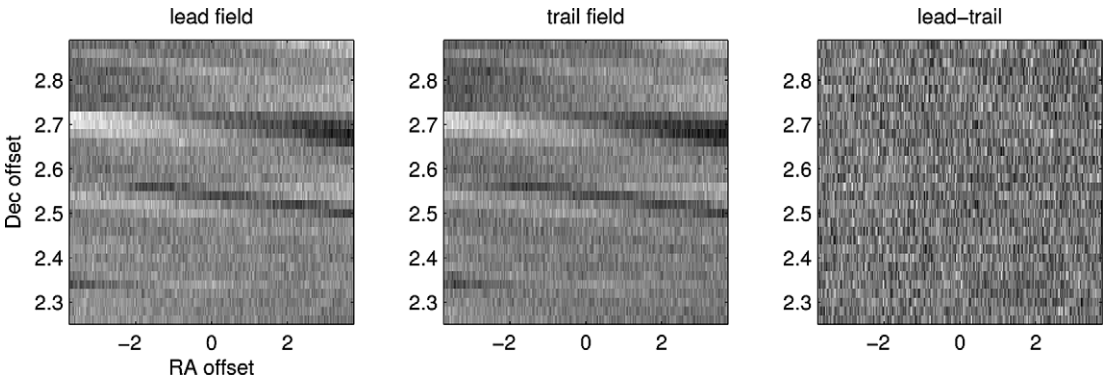

Fig. 10. Demonstration of the effectiveness of polarized ground pickup removal. The left and center panels show raw 8 h maps for the difference signal of a single detector pair on the lead and trail fields. *No filtering has been applied to this data—each row of pixels is simply four scans binned together*. The stripes across the map are due to polarized ground emission, which cancels to high precision in the lead-trail difference map shown at right.

is highly effective at removing it. The crucially important removal of pickup in the polarized case is shown in Fig. 10.

5. Observation strategy

Observations start at the same LST each day and our observation strategy includes the followings steps:

- A 5 min scan-set consists of scanning the telescope forwards then backwards, repeated four times. Each scan is superimposed on top of the general motion of the telescope tracking the field center.
- The elevation is changed by 0.02° and the scan-set repeated. In this way, a raster map of the sky is built up.
- After 30 min of scanning we switch to the trailing field and repeat the exact same pattern of scanning with respect to the ground.
- After 8 h the cryostat and telescope are rotated by 60° (termed a deck angle rotation) and the observations are repeated for a further 8 h.
- We perform a sky dip at the beginning of each day to cross-check atmospheric opacity values obtained from a 225 GHz tipper system located nearby. Four times each day we check the absolute pointing by scanning the center feed in a cross pattern over a bright galactic source.

This scan strategy has a high degree of redundancy and we can perform jack-knife tests by splitting data according to deck angle (azimuth range), and scan direction (forward or backward).

5.1. Status of the analysis of first year data

During the 2005 season we obtained a total of around 80 days of integration (after cuts for weather and instrument problems) on a total sky area of $10 \times 6°$. Our field is located in the deep field region observed by the 2003 flight of the Boomerang experiment (Masi et al.).

Two complete low level calibration/reduction and map making pipelines have been written, and the results cross checked at each stage. The following procedures are implemented: cosmic ray removal, deconvolution of detector time constants, low pass filtering and down-sampling of the data, gain matching of the bolometers (based on elnods), and finally building up co-added maps through the use of the measured feed offset angles, bolometer polarization angles and polarization efficiencies. The final product are maps of total intensity (T) and polarization (Q, U) for each of the two QUaD frequencies (100 and 150 GHz). Note that each half scan is polynomial filtered before being co-added into the map to remove large scale modes dominated by atmospheric fluctuations. In the left and center

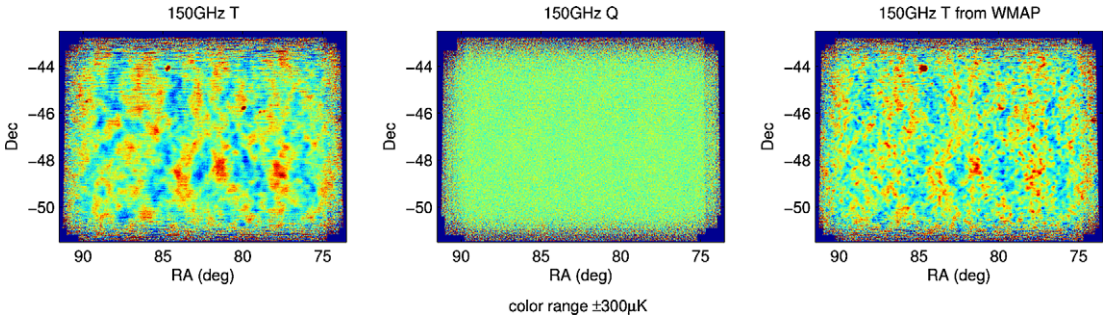

Fig. 11. The left and center panels show QUaD 1st season T and Q maps at 150 GHz, binned into fine (0.02°) pixels. Note the extremely high signal to noise we obtain for the degree angular scale T structure. At this pixelization the Q map is (white) noise dominated with an rms level of the Q (and U) maps of 30/20 μK per 0.02° pixel at 100/150 GHz. The right panel shows the three year WMAP map of our field processed through the QUaD simulation pipeline—see text for details.

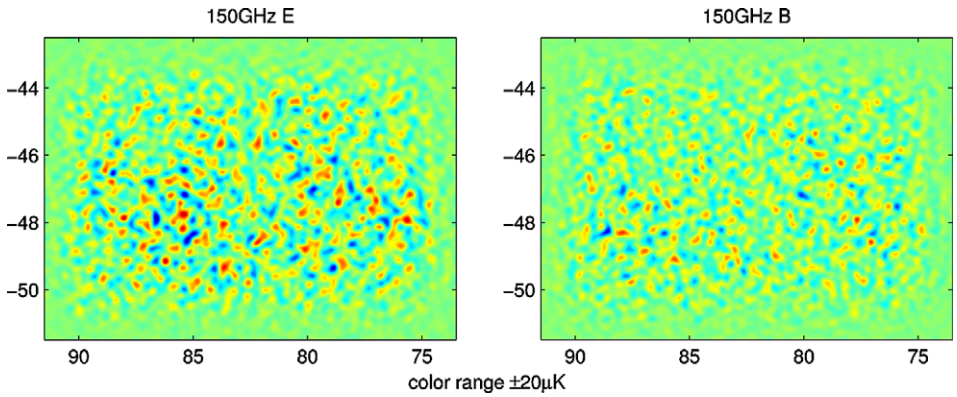

Fig. 12. QUaD first season polarization maps decomposed into E and B modes. Note that the E signal is much stronger than the B signal, as expected in the conventional cosmological model. Simulations indicate that the structure in the B map is consistent with instrumental noise alone.

panels of Fig. 11 we show T and Q maps at 150 GHz. These are finely pixelized maps and the Q map appears to be white noise. For the purposes of visual illustration we take the Q, U maps to the Fourier plane, convert to E and B, Weiner filter them (assuming LCDM) and go back to the map plane. The result of this procedure is shown in Fig. 12.

As a comparison to our results, the right-hand panel of Fig. 11 also shows the results of passing the WMAP 3 year T map through the QUaD simulation. The large scale structure shows excellent agreement, but at the smaller angular scales WMAP has far lower signal to noise than QUaD (which leads to the artificial impression that WMAP has higher angular resolution than QUaD). We are obtaining absolute calibration by applying the same procedure to the Boomerang 2003 map, which is itself cross-calibrated against the CMB dipole and checked against WMAP.

To correct for the effects of filtering, beams and noise on the derived power spectra we use an adaptation (Brown et al., 2005) of the MASTER technique (Hivon et al., 2002). A crucial element of this technique is the ability to generate full Monte-Carlo simulations of the experimental timestream. Again two completely independent simulation codes have been written and tested.

5.2. Checks for polarization systematics in the QUaD system

We have quantified the effects of non-idealities in QUaD polarization measurements and their uncertainties as described below.

- *Uncertainties in cross polar leakage*: A systematic difference between the true cross-polar leakage and the assumed value will introduce an uncertainty into the overall calibration of the final polarization power spectra. It does not cause more problematic effects such as E–B mixing. From the measurements described in Section 3, we find that the cross-polar leakage is very stable and can be estimated to ±1% uncertainty for a single pixel. We have simulated the effect of a randomly distributed ±3% uncertainty on the true value for each pixel and find that the error in the normalization of the derived power spectrum is less than 1%.
- *Uncertainties in the angles of the PSBs*: Fig. 8 shows that the offsets of the angle of polarization of the individual detectors from the nominal directions is small (<3°). We have investigated the impact of this effect by simulating data with randomly scattered angles and reconstructing using the nominal angles, and find a negligible change in the results.
- *Differences in the two beams from a single pixel*: From beam mapping runs we find that the two A and B beams within each pair are offset by a fraction of an arcminute, resulting in a dipole pattern when the difference is taken—the mechanism for this effect is not yet understood. We include this effect in our simulations and find that the level of E-mode to B-mode mixing that it generates is negligible compared to our sensitivity. Analytic calculations confirm this result.

6. Conclusions

The QUaD experiment performed well during its first season of operation. Improvements have been made and we are now well into a second successful season. The response of the instrumental system has been characterized in some detail and analysis of the CMB data is in an advanced state. Results on the polarization power spectrum of the CMB which improve considerably on existing results will be released in the near future.

Acknowledgements

We would like to thank the NSF Office of Polar Programs and the staff of the entire United States Antarctic Program. QUaD is supported by a collaborative research grant from the NSF and by PPARC in the UK.

References

Brown, M.L., Castro, P.G., Taylor, A.N., 2005. Cosmic microwave background temperature and polarization pseudo-C_l estimators and covariances. MN-RAS 360, 1262–1280.

Bussmann, R.S., Holzapfel, W.L., Kuo, C.L., 2005. Millimeter wavelength brightness fluctuations of the atmosphere above the South Pole. ApJ 622, 1343–1355.

Cahill, G., O'Sullivan, C., Murphy, J.A., Lanigan, W., Gleeson, E., Ade, P.A.R., Bock, J.J., Bowden, M., Carlstrom, J.E., Church, S.E., Ganga, K., Gear, W., Harris, J., Hinderks, J., Hu, W., Kovac, J., Lange, A., Leitch, E.M., Maffei, B., Mallie, O., Melhuish, S., Orlando, A., Pisano, G., Piccirillo, L., Pryke, C., Rusholme, B., Taylor, A., Thompson, K.L., Zemcov, M., 2004. The quasi-optical design of the QUaD telescope. In: Zmuidzinas, J., Holland, W.S., Withington S. (Eds.), Astronomical Structures and Mechanisms Technology. In: Antebi, Joseph, Lemke, Dietrich (Eds.), Proceedings of the SPIE, vol. 5498, pp. 396–406.

Hivon, E., Górski, K.M., Netterfield, C.B., Crill, B.P., Prunet, S., Hansen, F., 2002. MASTEr of the cosmic microwave background anisotropy power spectrum: a fast method for statistical analysis of large and complex cosmic microwave background data sets. ApJ 567, 2–17.

Hu, W., White, M., 1997. A CMB polarization primer. New Astronomy 2, 323–344.

Jones, W.C., Bhatia, R., Bock, J.J., Lange, A.E., 2003. A polarization sensitive bolometric receiver for observations of the cosmic microwave background, In: Phillips, T.G., Zmuidzinas J. (Eds.), Millimeter and Submillimeter Detectors for Astronomy. In: Phillips, Thomas G., Zmuidzinas, Jonas. (Eds.), Proceedings of the SPIE, vol. 4855, pp. 227–238.

Kovac, J.M., Leitch, E.M., Pryke, C., Carlstrom, J.E., Halverson, N.W., Holzapfel, W.L., 2002. Detection of polarization in the cosmic microwave background using DASI. Nature 420, 772–787.

Kuo, C.L., Ade, P.A.R., Bock, J.J., Cantalupo, C., Daub, M.D., Goldstein, J., Holzapfel, W.L., Lange, A.E., Lueker, M., Newcomb, M., Peterson, J.B., Ruhl, J., Runyan, M.C., Torbet, E., 2004. High-resolution observations of the cosmic microwave background power spectrum with ACBAR. ApJ 600, 32–51.

Lee, C., Ade, P.A., Haynes, C.V., 1996. Self-supporting filters for compact focal plane designs. In: Rolfe, E.J., Pilbratt, G. (Eds.), ESA SP-388: Submillimetre and Far-Infrared Space Instrumentation, 1996, p. 81.

MacTavish, C.J., Ade, P.A.R., Bock, J.J., Bond, J.R., Borrill, J., Boscaleri, A., Cabella, P., Contaldi, C.R., Crill, B.P., de Bernardis, P., De Gasperis, G., de Oliveira-Costa, A., De Troia, G., Di Stefano, G., Hivon, E., Jaffe, A.H., Jones, W.C., Kisner, T.S., Lange, A.E., Lewis, A.M., Masi, S., Mauskopf, P.D., Melchiorri, A., Montroy, T.E., Natoli, P., Netterfield, C.B., Pascale, E., Piacentini, F., Pogosyan, D., Polenta, G., Prunet, S., Ricciardi, S., Romeo, G., Ruhl, J.E., Santini, P., Tegmark, M., Veneziani, M., Vittorio, N., 2006. Cosmological Parameters from the 2003 flight of BOOMERANG. Astrophys J 647, 799.

Masi, S., Ade, P., Bock, J., Bond, J., Borrill, J., Boscaleri, A., Cabella, P., Contaldi, C., Crill, B., de Bernardis, P., De Gasperis, G., de Oliveira-Costa, A., De Troia, G., Di Stefano, G., Ehlers, P., Hivon, E., Hristov, V., Iacoangeli, A., Jaffe, A., Jones, W., Kisner, T., Lange, A., MacTavish, C., Marini-Bettolo, C., Mason, P., Mauskopf, P., Montroy, T., Nati, F., Nati, L., Natoli, P., Netterfield, C., Pascale, E., Piacentini, F., Pogosyan, D., Polenta, G., Prunet, S., Ricciardi, S., Romeo, G., Ruhl, J., Santini, P., Tegmark, M., Torbet, E., Veneziani, M., Vittorio, N. Instrument, Method, Brightness and Polarization Maps from the 2003 flight of BOOMERanG, ArXiv Astrophysics e-prints.